EXPERIMENTAL INVESTIGATION OF CHAIN TENSION AND ROLLER SPROCKET IMPACT FORCES IN ROLLER CHAIN DRIVES

James C. Conwell
Department of Mechanical Engineering
Louisiana State University
Baton Rouge, LA 70803

G. E Johnson
Design Laboratory
Mechanical Engineering and Applied Mechanics
University of Michigan
Ann Arbor, MI 48109-2125

ensm

UMR1148

DESIGN, CONSTRUCTION, AND INSTRUMENTATION OF A MACHINE TO MEASURE TENSION AND IMPACT FORCES IN ROLLER CHAIN DRIVES[1]

James C. Conwell
Department of Mechanical Engineering
Louisiana State University
Baton Rouge, LA 70803

G. E. Johnson
Design Laboratory
Mechanical Engineering and Applied Mechanics
University of Michigan
Ann Arbor, MI 48109-2125
Glen_E._Johnson@um.cc.umich.edu

ABSTRACT

Most previous experimental investigations of chain drive dynamics have been completed on the classical four-square test machine (also referred to as a chain speeder in the industry). In this paper we discuss the design and construction of a new test machine configuration that offers some advantages over the traditional design. The new machine and attendant instrumentation provide more realistic chain loading, and allow link tension and roller - sprocket impact monitoring during normal operation. The incorporation of an idler sprocket allows independent adjustment of test span length and preload. The angle at which rollers approach an instrumented sprocket can also be adjusted. Drawbacks of the new configuration (compared to the four-square design) are that the support structure may not be as rigid and the additional sprockets (idler sprocket and instrumented sprocket) add kinematic complexity.

---

[1]This paper is based on the Ph.D. dissertation research conducted by the first author under the direction of the second author at Vanderbilt University, completed in December 1989.

NOMENCLATURE

a	Pitch Angle of a Sprocket
e(t)	Time response of a dynamic system
h(t)	Time-based transfer function of a dynamic system
i(t)	Time-based input to the dynamic system
E(w)	Frequency response of a dynamic system
H(w)	Frequency domain transfer function
I(w)	Frequency input to the dynamic system

INTRODUCTION

Chain drives are among the oldest of the basic machine elements. In spite of their widespread use, in 1984 Freudenstein observed that were not well understood. Freudenstein's observations, coupled with the desire on the part of the auto industry to better understand chain drives in order to reduce engine and power transmission development time, have lead to a renaissance in theoretical and experimental investigation, including studies by Chen and Freudenstein (1988), Wang (1992), Wang et al (1992), Kim (1990), Kim and Johnson (1992a and 1992b), Choi and Johnson (1992a and 1992b), Conwell, Johnson, and Peterson (1992a, 1992b, 1992c), and Veikos and Freudenstein (1992a and 1992b).

Chain drive dynamics became of interest to the automobile industry with the rise in importance of *noise, vibration, and harshness* (NVH). Chain drives offer non-slip, light weight, inexpensive, compact power transmission compared to belts or gears, but usually at the cost of increased noise and vibration. A brief history of chain drives and the important milestones in their practical development through the late twentieth century can be found in Conwell (1989).

Today, three types of chains are commonly found: roller chains, silent chains and engineering steel chains. The new test machine was designed specifically to investigate roller chains, so the remainder of this discussion will be limited to chains of this type. Chain drives were poorly understood through the 1980's for a variety of reasons, including the polygonal action, nontrivial sprocket geometry, intentional clearances and unintentional dimensional variations due to manufacturing tolerances, friction, and the large number of bodies that make up the typical chain and sprocket system.

The manufacture of roller chains has been standardized by the American National Standards Institute under standard B29.1 (ANSI, 1972) since 1913. The first report in an ASME journal devoted to the study of roller drive chain behavior was given by Bartlett (1935). Bartlett developed a new approach to rating roller chain drives based upon sprocket impact loads and experience. Bremer (1947) reported on marine applications and analyzed the various loads on chain drives. Staments (1951) considered the fundamental loads on chain drives using an optical strain gage. Most modern work can be directly traced to Binder's (1956) classical text. In his work, Binder both documented and extended the work of many early chain investigators.

Polygonal action has been one of the most studied chain drive topics. Morrison (1952), Mahalingham (1952), Okoshi and Uehara (1959a and 1959b) and Bouillon and Tordion (1965) all reported on this phenomenon.

Ryabov (1968) and Chew (1985) modeled the inertia effects on impact forces in chain drives, while Radzimovsky (1955) developed an 'equalizing' linkage in an attempt to minimize the impact. Turnbull and Fawcett (1975) completed an approximate kinematic analysis of roller chain drives.

Recent research on chain drives has been conducted at the University of Michigan (Johnson), Pennsylvania State University (Wang), University of Texas (Marshek), Chalmers University of Technology (Gerbert) and Columbia University (Freudenstein). Marshek and his students (1978, 1982, 1983a, and 1983b) determined quasi-static chain and sprocket load distributions. Chen and Freudenstein (1988) completed an approximate kinematic analysis of the roller chain drive. Veikos and Freudenstein (1992a and 1992b) developed a lumped mass dynamic model based on Lagrange's equations of motion and also studied chain drive vibrations. Wang's work is based on a continuous model of the axially moving material and he has studied the stability of chain spans subject to periodic

sprocket excitations (Wang 1992) and the effect of impact intensity on chain drive vibrations (Wang, et al, 1992). Gerbert studied the tooth load distribution of seated and unseated roller chains and timing belts and made several important observations about the effects of friction and elasticity. Kim and Johnson (1992a and 1992b) developed a detailed model of the roller - sprocket contact mechanics that allowed the first determination of actual pressure angles and a multi-body dynamic simulation based on Kane's dynamic equations. Choi and Johnson (1992a and 1992b) incorporated the effects of impact, polygonal action, and chain tensioners into the axially moving material model and studied transverse vibration of chain spans.

Much work has been completed, but much work remains. The remainder of this article is devoted to the physical description of our test machine, along with its attendant general purpose instrumentation.

CHAIN DRIVE EVALUATION MACHINE

Design of the New Test Machine

The new test machine was designed to load the chain drive up to three horsepower over a wide range of chain speeds, with adjustable center distance between sprockets, and with an adjustable angle of approach for engagement of the chain with an instrumented sprocket.

An assembly drawing of the test machine is presented in Figure 1. Table 1 contains a list of components of the test machine, with letters referenced in Table 1 corresponding to parts located in Figure 1. A primary advantage of the new load scheme and geometry is that the center distance in one of the chain spans is independent of chain tension. The length can be measured with a pair of machinist's dividers and adjusted as required. Another advantage is that an instrumented idler with adjustable angle of approach can measure the dynamic interactions between rollers and sprocket teeth. A third advantage of the design is that it allows overhung sprocket mounting so that a strain gage can be mounted on a link side plate and can be connect with a wiring harness to strain monitoring instrumentation.

Drive Train

The test machine is powered by a three-phase, 208 volt, three horsepower electric motor (K). The drive shaft of the test machine is supported by a welded steel bracket (G) and is driven by the motor through a V-Belt (I) and sheave (F). The motor is mounted on an adjustable frame (H). The adjustable base can accommodate different size motor drive shaft sheaves; different drive sheaves provide different linear chain speeds. Furthermore, the frame allows quick adjustment of the drive belt tension to compensate for any belt stretch that may occur.

The motor mounts were selected to reduce transmission of shock to the motor base. The motor has a 'no-load' operating speed of 1740 revolutions per minute. On/off control of the motor is accomplished by a NEMA size 0 motor starter (AA).

Chain Loading

Preloading the chain is accomplished through the use of an idler/tensioner sprocket assembly (V). This assembly consists of a twelve tooth idler sprocket, a load cell and an adjustment track which permits the vertical location of the center line of the sprocket to be varied. The load cell is an integral part of the assembly and can instantly measure the vertical force being applied to the shaft of the idler/tensioner sprocket.

The preload chain tension was calibrated as a function of the output of the integral load cell. During experiments, once the desired preload tension is reached, the idler/tensioner assembly is locked into position.

The power transmission component of the chain load is obtained by placing external loads on the resistive shaft (X). A sheave (W) is mounted on the resistive shaft. This pulley, via a V-belt (L), drives a countershaft assembly (M,P) which in turn drives a 60 ampere automobile alternator (S). The countershaft assembly allows the alternator to turn at a higher speed than the resistive shaft. Furthermore, by changing the pulleys mounted on the countershaft (M), it is possible to maintain a constant speed of the alternator. This arrangement allows tests to be conducted for a range of linear chain speeds with constant torque transmission.

To vary the torque transmitted by the test chain drive, electricity produced by the alternator is passed through a load box with 15 three ohm switched resistors wired in parallel. The torque transmitted by the chain (and required to rotate the resistive sprocket) can be varied by altering the number of resistors switched into the alternator circuit. During the operation of the test machine, the speed of the alternator is 4500 RPM. The alternator produces approximately 13.6 V DC at this speed.

The vertical location of the resistive shaft assembly can be varied. The shaft assembly can be moved along the vertical support (J), while the support arm (U) can be slid along the main support beam (Z), permitting the use of a variety of test sprockets (D), while maintaining the horizontal aspect of the upper chain span. Additionally, the horizontal position of the resistive shaft can be varied, although it was maintained in a fixed position throughout the experiments.

Chassis and Frame

The baseplate of the machine (N) is cold-rolled, quarter-inch thick steel plate, while the main structural members (Z) are three-inch I beams. These materials were chosen for their stiffness, their good machining characteristics and their low cost. The main structural members are welded together and bolted to the base plates.

The resistive shaft assembly (Y) is mounted on a structure of 3/4-inch cold-rolled round steel members (J) and (U). The center distance between the resistive sprocket and the test sprocket (D) can be adjusted, as can the height of the resistive sprocket. The drive shaft, the countershaft and the resistive shaft are supported by 3-inch wide, 3/8-inch hot rolled steel plates. All of the shafting in the test machine is constructed of 5/8-inch cold rolled steel rounds, chosen for both strength and surface finish.

Test Machine Instrumentation

An IBM 80286 based computer with 80287 math coprocessor is used to control and monitor the experiments through an IBM Data Acquisition and Control Adapter (IBM DACA board) and an IBM General Purpose Interface Bus Adapter (IBM GPIB board).

The primary use of the DACA board is the determination of the rotation speed of the instrumented sprocket (D). A photon coupled interrupter module is placed across the instrumented sprockets so that the teeth of the sprocket intermittently block the beam across the interrupter as the sprocket rotates. The output of the interrupter module is 0.8 V DC when the beam is not blocked, but rises very quickly to 6.0 V DC once the beam is blocked. The DACA board is used to both power and monitor the voltage output of the photon interrupter. If the number of teeth on the instrumented

instrument and the sampling rate of the DACA board are known, then the speed of the instrumented sprocket can be readily determined. The GPIB is defined by ANSI/IEEE Standard 488-1978.

The data were collected with the aid of a Bruel and Kjaer (B&K) 2032 dual channel spectrum analyzer. This analyzer can be totally controlled via the GPIB bus. Serial polls can be requested from the 2032, providing a means of updating status as well as error checking. One of the most useful capabilities of the 2032 is the ability to store a data file of measurement results in an external storage medium (e.g., the hard drive on a computer). The 2032 has the capability to perform real-time analysis as well as process previously collected data.

Tension Monitoring

The tension in a link is monitored by means of a strain gage mounted on the link side plate (a quarter bridge). The strain gage is connected to a Vishay/Ellis (V/E) 20A Digital Strain Indicator by a wiring harness to condition the output of the strain gage. The features of the V/E 20A are an isolated DC power supply for gage excitation, bridge completion circuits to achieve initial bridge balance and calibration, a fixed gain DC differential amplifier and a digital voltmeter readout.

The V/E 20A has excellent shielding and is almost immune to electrical noise common found in the vicinity of motors and other electronic equipment. The V/E 20A output (plus or minus 5 volts DC) can be fed directly from the strain indicator to the B&K 2032. Figure 3 presents a schematic drawing of the instrument connections for the chain tension experiments.

The tension on each link varies throughout the operation of the chain drive. A gross variation occurs as the chain moves from the tight span to the loose span and back again. High frequency variation occurs due to impact, and span stiffness and span length variations that take place as the rollers engage and disengage with the sprockets. It is likely that this cyclic loading of the links strongly affects chain life descriptors like stretch, wear, and fatigue, and other performance descriptors like noise and vibration.

Impact Monitoring

To illustrate the mechanism of impact in roller chain drives, Figure 2 shows a chain wrapping around a sprocket. Roller A is shown seated on the sprocket. As the sprocket continues to turn, the chain link joining rollers A and B articulates about the pin joint of roller A. After the sprocket has rotated an angle equal to the pitch angle of the sprocket (a), roller B approaches and impacts the sprocket at the next subsequent tooth recess. As the sprocket continues to turn, this event repeats itself. The magnitude of the impulsive force at impact is numerically equal to the product of the effective mass (the mass involved in the impact), the relative velocity between a roller and the sprocket tooth recess and the reciprocal of the time for the event to occur. In order to measure the impact force, an instrumented sprocket support and frame was incorporated into the machine.

Referring again to Figure 1, this instrumented sprocket assembly is indicated by the letters A, B and C with the actual instrumented sprocket as letter D. Each of the instrumented sprocket brackets are two-force members, joined to the main superstructure of the machine and to each other with pin-joints. As two-force members, they can only transmit loads applied along their length. The two support brackets are arranged orthogonally with respect to each other. Each of the support brackets has a load cell included as an integral part of the bracket. As a roller element seats onto the instrumented sprocket (D), an impact force occurs. This impact force is immediately resolved into the two orthogonal directions (horizontal and vertical) through the use of the two force members, while the magnitude of the force in each direction is determined by the load cell.

Each load cell is an aluminum ring with four strain gages. Two of the gages are mounted on the exterior of the ring and two on the interior in order to increase load cell output and sensitivity. The output from each load cell is fed into a Vishay-Ellis 20A digital strain indicator, which also provides the excitation for the strain gage bridge. The output of the strain indicators is then fed into the B&K 2033 (the signal from the vertical load cell is monitored by Channel A and the signal from the horizontal load cell is monitored by Channel B).

The photocell is powered by the IBM computer and its output during the experiment is monitored by the DACA board. Additionally, the computer controls the spectrum analyzer throughout the experiment. Figure 4 presents a schematic drawing of the instrument connections for the impact force experiments.

Determination of the Impact Input Force From Measurement of the Output Spectra

The response of virtually any linear system can be related to the system input through a transfer function. In the time domain, this relationship can be expressed as:

$$e(t) = \int_0^t i(t)h(t - t)dt \qquad (1)$$

where e is the response of the system, h is the impulse response or unit sample response, and i is the system input. In the frequency domain, equation (1) becomes:

$$E(w) = H(w) * I(w) \qquad (2)$$

It is customary to work with equation (2), i.e., in the frequency domain. If the input to the system is known, then the response of the system can be measured. It is then a simple matter to deduce the system transfer function. The transfer functions for both the horizontal and vertical load rings were experimentally determined by this strategy. In experiments, the system response can be measured, and the known system transfer functions can then be used to deduce the input excitation, i.e., the impact force associated with the conditions of the experiments.

Conversion Of The Machine From Tension Measurement to Impact Measurement

The sprocket support structure can be changed from an arrangement where the sprockets are supported by one bearing on each side to an arrangement where the sprocket is overhung. In the first position the impact force can be measured. In the overhung position, the wiring harness from the link side plate strain gage is free to move around the chain span (at least until the helix that the wires wind themselves into is ready to fail - on the order of one minute). This allows the tension measurement. A General Electric H21B1 photon coupled interrupter module is used as a locator device in order to provide a reference point for each data cycle. A sketch of the experimental setup is shown below, followed by a representative strain gauge output data.

SUMMARY

In this paper we have presented the essential features of the new test machine. The new machine offers significant advantages that allow more data collection options than have been

traditionally available. Data obtained with the new test machine will be reported in another article and can also be found in Conwell (1989).

ACKNOWLEDGMENT

After the test machine had been built, the National Science Foundation provided support for experiments through grants no. MSM-88-12957 and MSS-89-96293. This support is gratefully acknowledged.

REFERENCES

American National Standards Institute, 1972, "Transmission Roller Chains and Sprocket Teeth," ANSI Standard B29.1, New York, NY.

Bartlett, G.M., 1935, "A New Basis for the Rating of Roller Chain Drives," Trans. ASME, V. 57, Number 3, pp. 97.

Binder, R.C., 1956, Mechanics of the Roller Chain Drive, Prentice-Hall, Englewood Cliffs, NJ.

Bouillon, G., and Tordion, G.V., 1965, "On Polygonal Action in Roller Chain Drives," Trans. ASME J. Engineering for Industry, V. 87B, pp. 243-250.

Bremer, N.C., 1947, "Heavy Duty Chain Drives for Marine Propulsion Service," Trans. ASME, V. 69, pp. 441-452.

Chen, C-K, and Freudenstein, F., 1988, "Toward a More Exact Kinematics of Roller Chain Drives," Trans. of the ASME J. Mechanisms, Transmissions and Automation in Design, V. 110, No. 3, pp. 269-275.

Chew, M., 1985, "Inertia Effects of a Roller-Chain on Impact Intensity," Trans. ASME J. Mechanisms, Transmissions and Automation in Design, V. 107, pp. 123-130.

Choi, W. and Johnson, G. E., 1992a, Vibration of Roller Chain Drives at Low, Medium and High Operating Speeds, MEAM Technical Report Number 92-08, University of Michigan, Ann Arbor, Michigan.

Choi, W. and Johnson, G. E., 1992b, Transverse Vibrations of a Roller Chain Drive with Tensioner, MEAM Technical Report Number 92-09, University of Michigan, Ann Arbor, Michigan.

Conwell, J. C., 1989, An Examination of Transient Forces in Roller Chain Drives, Ph.D. Dissertation, Vanderbilt University, Nashville, TN.

Eldiwany, B.H. and Marshek, K.M., 1984, "Experimental Load Distributions for Double Pitch Steel Roller Chains on Steel Sprockets," Mechanism and Machine Theory, Volume 19, Number 6, pp. 449-457.

Freudenstein, F., 1984, "Machine Dynamics: Some Thoughts on Research Initiatives," Trans. ASME J. Mechanisms, Transmissions, and Automation in Design, V. 106, No. 3, pp 264 - 266.

Gerbert, G., et al, 1978, "Load Distribution in Timing Belts," Trans. ASME J. of Mechanical Design, V. 100, pp. 208-215. TJ 230 .J86

Gerbert, G., 1989, "Tooth Action in Chain and Timing Belt Drives," Proceedings of the International Power Transmission and Gearing Conference, Volume 1, ASME, Book 10288A - 1989, pp 81 - 89.

Kim, M. S., 1990, Dynamic Behavior of Roller Chain Drives at Moderate and High Speeds, Ph.D. dissertation, University of Michigan.

Kim, M. S., and Johnson,G. E., 1992a, Mechanics of Roller Chain-Sprocket Contact, MEAM Technical Report Number 92-06, University of Michigan, Ann Arbor, Michigan.

Kim, M. S., and Johnson, G. E., 1992b, A General Multi-Body Dynamic Model to Predict the Behavior of Roller Chain Drives at Moderate and High Speeds, MEAM Technical Report Number 92-07, University of Michigan, Ann Arbor, Michigan.

Mahalingam, S., 1858, "Polygonal Action in Chain Drives," J. Franklin Institute, Number 1, pp. 23-28.

Marshek, K.M., 1978, "On the Analyses of Sprocket Load Distribution," Mechanism and Machine Theory, Volume 14, pp. 135-139. TJ 1 .J87

Morrison, R.A., 1952, "Polygonal Action in Chain Drives," Machine Design, Volume 24, pp. 155-159.

Naji, M. and Marshek, K.M., 1983a, "Analysis of Sprocket Load Distribution," Mechanism and Machine Theory, Volume 18, Number 5, pp. 349-356.

Naji, M. and Marshek, K.M., 1983b, "Experimental Determination of the Roller Chain Load Distribution," Trans. ASME J. Mechanisms, Transmissions and Automation in Design, V. 105, pp. 331-338.

Okoshi, M. and Uehara, K., 1959a, "Study on the Uneveness of Transmission Roller Chains, First Report," Journal of the Japan Society of Precision Engineering, Volume 25, Number 9, pp. 425-431.

Okoshi, M. and Uehara, K., 1959b, "Study on the Uneveness of Transmission Roller Chains, Second Report," Journal of the Japan Society of Precision Engineering, Volume 25, Number 10, pp. 552-558.

Radzimovsky, E.I., 1955, "Eliminating Pulsations in Chain Drives," Product Engineering, Volume 26, pp. 153-157.

Ross, M.O. and Marshek, K.M., 1982, "Four-Square Sprocket Test Machine," Mechanism and Machine Theory, Volume 17, Number 5, pp. 321-326.

Ryabov, G.K., "Inertial Effects of Impact Loading in Chain Drives," Russian Engineering Journal, Volume 48, Number 8, pp. 17-19.

Staments, W.K., 1951, "Dynamic Loading of Chain Drives," Trans. ASME, July 1951, pp. 655-665.

Turnbull, S.R., and Fawcett, J.N., "An Approximate Kinematic Analysis of the Roller Chain Drive," Proceedings of the Fourth World Congress on Theory of Machines and Mechanisms, pp. 907-911.

Veikos, N. C. and Freudenstein, F. 1992a, "On the Dynamic Analysis of Roller Chain Drives : Part 1- Theory", Mechanism· Design and Synthesis, DE-vol. 46, edited by Kinzel et al, ASME, NY, 1992, pp.431-438.

Veikos, N. C. and Freudenstein, F., 1992b, "On the Dynamic Analysis of Roller Chain Drives: Part 2,", Mechanism Design and Synthesis, DE-vol. 46, edited by Kinzel et al, ASME, NY, 1992, pp.439-450.

Wang, K. W., 1992, "On the Stability of Chain Drive Systems Under Periodic Sprocket Oscillations," Trans. ASME J. Vibration and Acoustics, Vol. 114, pp 119 - 126.

Wang, K. W., et al, 1992, "On the Impact Intensity of Vibrating Axially Moving Roller Chains," Trans. ASME J. Vibration and Acoustics, Vol. 114, pp 397 - 403.

TABLE 1
PARTS LIST FOR THE CHAIN TEST MACHINE

Part Letter	Part Description
A	Strain Gauge/Load Ring Assembly
B	Isolated Sprocket Bracket
C	Isolated Sprocket Support
D	Mechanically Isolated Sprocket
E	Drive Sprocket
F	Drive Pulley
G	Drive Shaft Support Assembly
H	Electric Motor Adjustable Base
I	Drive Belt
J	Resistive Sprocket Vertical Support
K	3 HP Electric Motor
L	Countershaft Drive Belt
M	Countershaft Pulleys
N	Machine Base plates
O	I-Beam Horizontal Supports
P	Countershaft Support Assembly
Q	Alternator Drive Bracket
R	Alternator Support Bracket
S	Alternator
T	Resistive Sprocket Support Plate
U	Resistive Sprocket Support Arm
V	Idler/Tensioner Sprocket Assembly
W	Countershaft Drive Pulley
X	Resistive Sprocket
Y	Resistive Pulley Shaft Support
Z	Main Superstructure Support Beam
AA	NEMA Size 0 Motor Starter

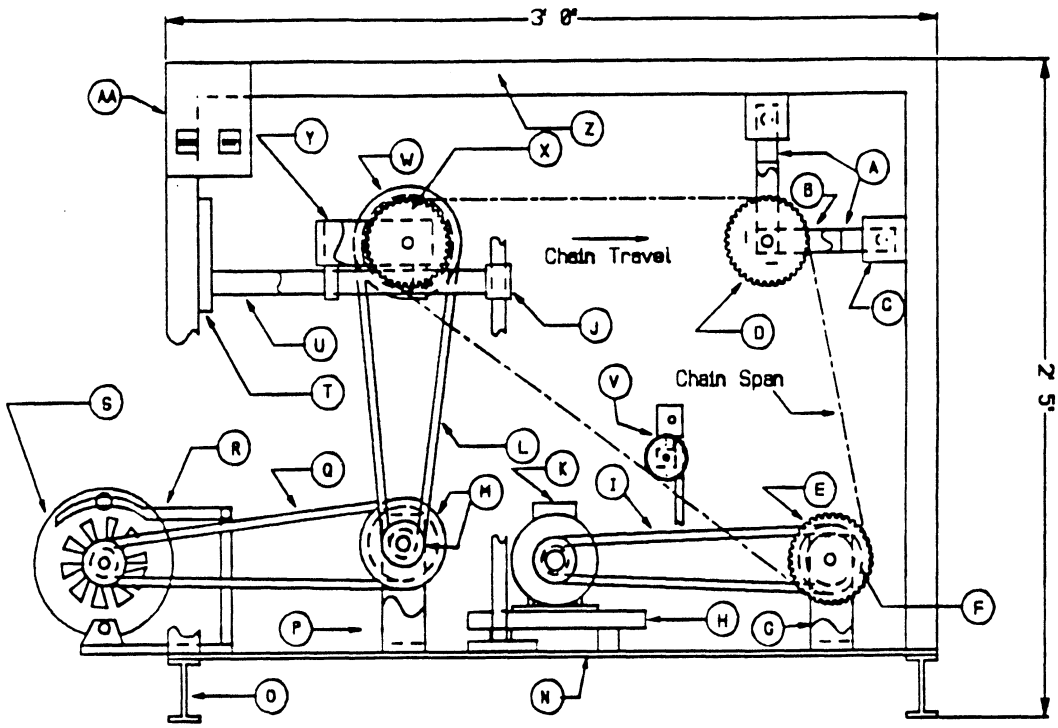

Figure 1. Schematic drawing of the new test machine.

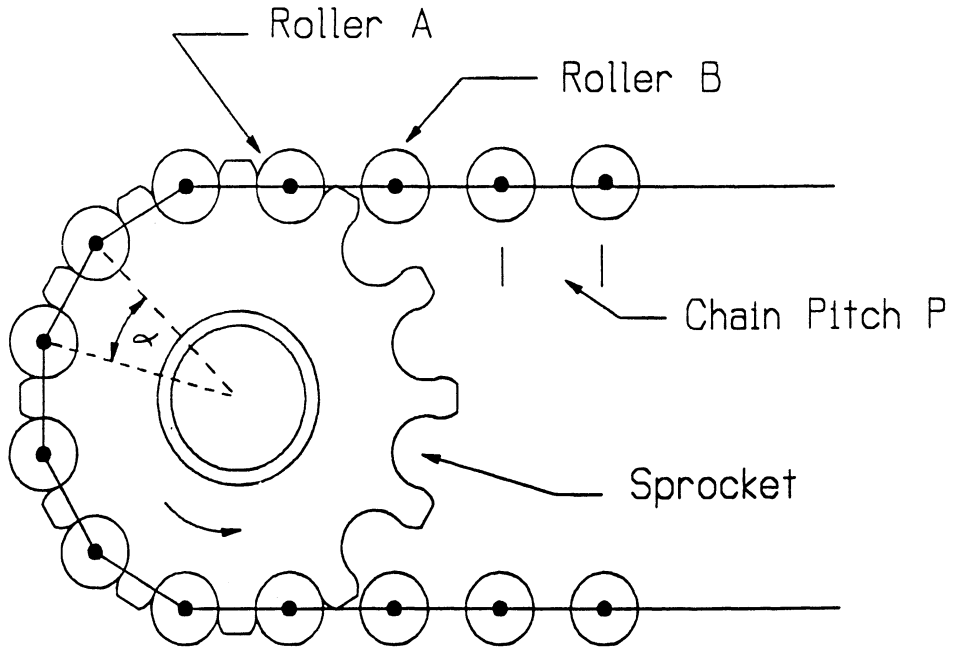

Figure 2: Roller B is about to seat, causing an impact force between roller B and the sprocket.

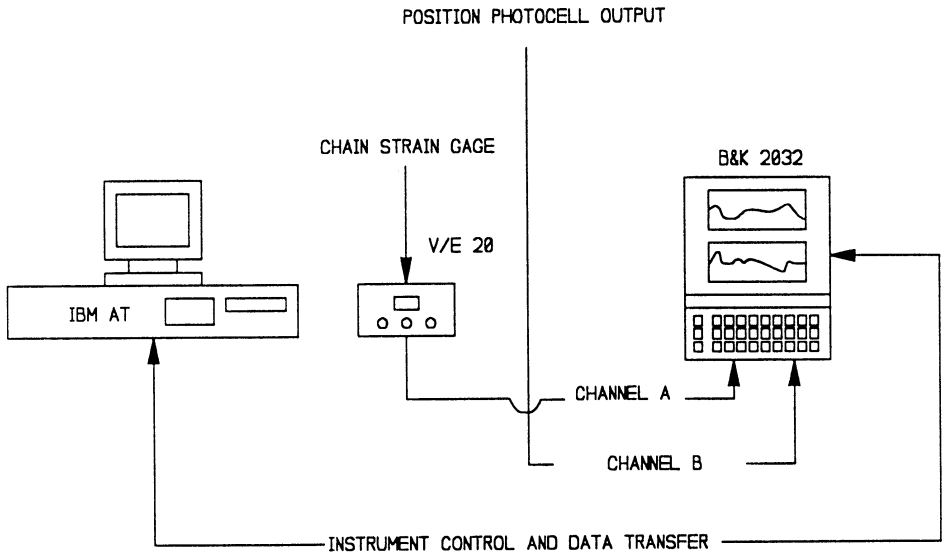

Figure 3: Schematic drawing of the instrumentation for the measurement of the chain tension.

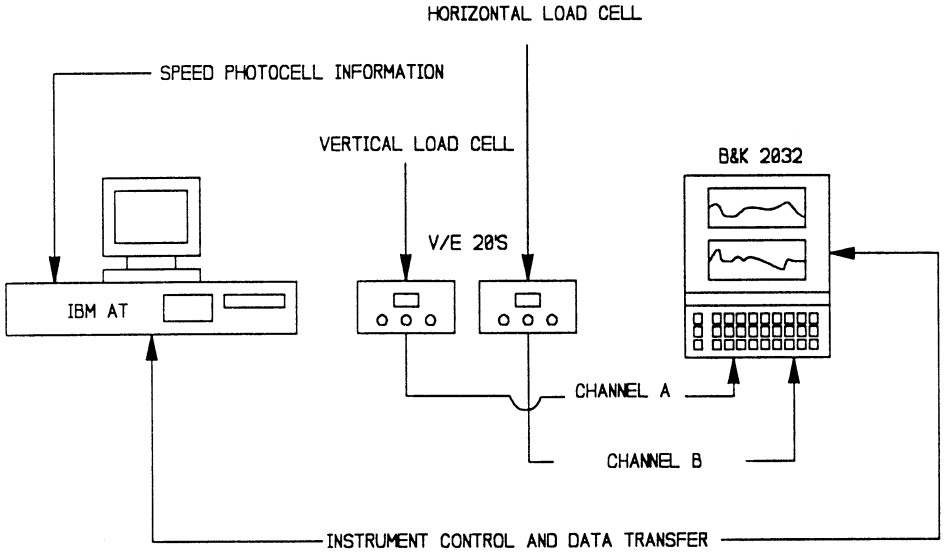

Figure 4: Schematic drawing of the instrumentation for the measurement of the impact force.

Experimental Investigation of Link Tension and Roller - Sprocket Impact in Roller Chain Drives

James C. Conwell[1]
Department of Mechanical Engineering
Louisiana State University
Baton Rouge, LA 70803

G. E. Johnson
Design Laboratory
Mechanical Engineering & Applied Mechanics
University of Michigan
Ann Arbor, MI 48109-2125

ABSTRACT

This paper presents the results from a recent experimental investigation into the dynamic behavior of roller chain drives. A strain gage mounted on a link side plate was used to measure the force in the link side plate during normal operation over a wide range of linear chain speeds and preloads. The test machine also included a specially instrumented idler sprocket that allowed the measurement of the horizontal and vertical components of the bearing reaction force. The roller - sprocket impact force was then determined with an experimentally determined transfer function approach facilitated by a Bruel & Kjaer 2032 dual channel spectrum analyzer. Observations about the data include:

- As is typically assumed, under quasi-static conditions, dynamic effects can be neglected without introducing significant error.
- As chain speed increases, dynamic effects become increasingly important.
- As is the case for belt drives, the average tight side chain tension can be expressed in the classical form of the preload, the driven load, and the load due to centrifugal force with only modest error over a wide range of linear chain speeds.
- The tension in a chain link increases very rapidly as the link exits the driven sprocket. The increase from loose side to tight side average tension occurs over less than two sprocket teeth.
- The tension in a chain link decreases very rapidly as the link enters the drive sprocket. The decrease from tight side to average loose side tension occurs over less than two sprocket teeth.
- Transient spikes are present in the tension data at the point where the link exits the driven sprocket and at the point where the link enters the driven sprocket.
- Impact force tends to increase as chain tension increases, however the relationship is not monotonic.

---

[1]This paper is based on the Ph.D. dissertation of the first author which was completed under the direction of the second author at Vanderbilt University, December 1989.

- Impact force tends to increase as chain speed increases, however the relationship is not monotonic.

- For a chain traveling in the horizontal direction, the vertical component of the impact force is much larger than the horizontal component.

- The magnitude of the horizontal component of the impact force increases more rapidly than the magnitude of the vertical component as the chain speed increases, indicating that the angle of impact (as measured from a vertical line) increases as chain speed increases.

INTRODUCTION

Several investigators have studied the forces that exist in a chain link during operation of the chain drive (Staments (1951), Radzimovsky (1955), Binder (1956), Ryabov (1968), Turnbull and Fawcett (1975), Naji and Marshek (1983a and 1983b), Eldiwany and Marshek (1984), Chew (1985), Chen and Freudenstein (1988), Wang (1992), Wang et al (1992), Kim and Johnson (1992a and 1992b), Choi and Johnson (1992a and 1992b), Veikos and Freudenstein (1992a and 1992b), and Gerbert (1978 and 1989)). As a link moves around the drive, the forces in the link vary. In the most general case, these forces go from a high level on the 'tight' side of the chain, reduce in magnitude as the link engages with and then rotates around the drive sprocket to the 'loose' side of the chain, and then increase in magnitude as the link moves around the driven sprocket and returns to the tight side. Furthermore, when a link leaves the span and engages with a sprocket, an impact force occurs due to the relative velocity between the roller and sprocket.

It has been proposed that these forces are responsible for the stretch, wear, fatigue, noise, and vibration that occur in chain drives. Until now these forces have never been experimentally measured throughout the link's cycle from tight to loose and back again. To enable direct measurements of the link tension and impact forces, a new test machine was designed and built. The design details and the instrumentation attendant to the machine are described in a companion article in this journal.

The experiments described here were completed with the new test machine and with standard ANSI number 40 riveted steel roller chain and 40B12 sprockets. Link tension data were collected first. Then the test machine was reconfigured and impact data were collected. In the remainder of this paper, the experimental methods and the data that were collected are presented and discussed.

For the purpose of this discussion, an experimental run is defined as an experiment conducted for a specific chain speed, dynamic chain loading, and chain preloading. An experimental group is all of the experimental runs conducted at a specific chain speed. An experimental group consists of 36 experimental runs. A total of four experimental groups (for a total of 144 experimental runs) were conducted. Data are tabulated in the Appendix.

More complete details of the experiments and instrumentation can be obtained by consulting Conwell (1989).

LINK TENSION

Procedure

The procedure developed to measure the chain side plate force is outlined below.

1. Set preload. Monitor output from the link side plate strain gauge.

2. Configure Bruel & Kjaer 2032 (B&K 2032).

3. Set resistance level for alternator circuit. Position photocell power on.

4. Place B&K 2032 in time history mode to act as high speed, high accuracy A/D converter.

5. Five seconds after B&K 2032 is placed in time history mode, turn on test machine. Run test machine for 30 seconds. Five seconds after test machine shut off, take B&K 2032 out of time history mode.

6. While B&K 2032 is in time history mode, write data to Intel 80286 based computer controlling the equipment. Once a particular experimental run is completed, place additional information in this data file concerning the time and date of the test and the overall status of the data.

7. Check data for existence of overload condition prior to beginning a new test. Overload indicates invalid test run. Discard data if overload was present.

8. Remove resistance from alternator and preload from chain.

The entire test procedure was automated and controlled by an Intel 80286 based personal computer. This facilitated repeatability and consistency. Once an experimental group was completed, the test machine was dismantled, the speed was changed, and all calibrations were checked. The machine was then reassembled in preparation for the next experimental group.

During the course of an experimental run, the link on which the strain gauge is mounted travels around the chain loop (from loose to tight and back again) many times. Data from the tight sight of the chain span were separated from the data collected on the loose side of the chain span. Average values for chain side plate force were determined for both the tight and loose spans.

Link Tension Data and Discussion

Figures 1a through 1d present the time averaged force in the tight side of the chain (as a function of torque transmitted) for the four linear chain speeds tested. These data can also be found in the Appendix in tabulated form. As would be expected, the data indicate that the addition of the preload tends to shift the tension in the tight side of the chain by the amount of the preload. The value of the tight side tension was predictably sensitive to the linear chain speed. For example, the time averaged tight side tension at a sprocket speed of 1400 rpm is approximately 8 pounds higher than the time averaged tight side tension at a sprocket speed of 800 rpm for comparable pre- and external loading.

Consider the free body diagram of the load sprocket shown in Figure 2. The model often posed for this case is simply

$$T_t = (M / R_p) + T_l \qquad (1)$$

where M is the external moment acting on the sprocket, R_p is the pitch radius of the sprocket, and T_t and T_l are the tight and loose side tensions respectively.

If the experimentally preset external moment, and the experimentally measured time averaged loose side tension are substituted into equation (1), it is possible to use equation (1) to predict the tight side tension. These calculated results are presented in juxtaposition with the experimentally measured time averaged values for tight side tension in Figures 3a through 3d.

The addition of a term that is proportional to the square of the linear chain speed allows fairly accurate prediction of the time averaged tight side tension, i.e.,

$$T_t = \text{Preload} + (M / R_p) + .00304wV^2 \qquad (2a)$$

where w is the weight per unit length of chain in pounds per inch, V is the linear speed of the chain in inches per second, and other terms are as defined before. The coefficient on the third term of equation (2a) was determined by regression analysis. If the weight per unit length in equation (2a) is replaced by the mass per unit length divided by the acceleration of gravity, the equation becomes

$$T_t = \text{Preload} + (M / R_p) + 1.17mV^2 \qquad (2b)$$

Incorporation of a term including the product of the mass per unit length and the square of the linear speed has been previously introduced to account for the centrifugal force in the general axially moving material problem (Mote, 1965). The constant of proportionality is dependent on the stiffness of the pulley (in this case sprocket) mounting system relative to the stiffness of the span of the moving material. For a simple single span system, the axially moving material model predicts that as the stiffness of the mounting becomes large relative to the stiffness of the span of moving material, the constant of proportionality approaches zero. As the stiffness of the mounting becomes small relative to the stiffness of the span of moving material, the constant of proportionality approaches unity.

The constant of proportionality in equation (2b) is greater than unity, but this does not violate any physical principals. Beikmann, Perkins, and Ulsoy (1992) have shown that values larger than unity are possible for belt systems with two pulleys and a tensioner. It is even possible to predict negative constants of proportionality for some geometric configurations, indicating the presence of a static instability.

Another possible explanation for the large constant of proportionality is the fact that there is no place for the effects of impact to be introduced in this model, except through the centrifugal force term. Accordingly, the constant of proportionality for the centrifugal force term will tend to be overestimated.

Prediction of the constant of proportionality has been historically difficult. Typically, some approximate value has been assumed based on "experience." General guidelines which give approximate values for the constant of proportionality as a function of chain type, chain span, and qualitative mounting structure details would be useful and should be the subject of a future investigation. The study by Beikmann, Perkins, and Ulsoy (1992) is a seminal step toward realization of this goal.

Load Distribution on the Sprockets

The way that the chain force changes as the link moves from either span onto and around either sprocket has long been of interest. Binder (1956) was the first to formally report on this phenomenon. Marshek et al. (1984) presented load distribution data for quasi-static experiments. Kim and Johnson (1992a and b) present an analytical model that very accurately maps the data reported in Marshek et al. (1984). In the present study, realistic chain speeds were used, and dynamic effects were clearly important. Inertial effects, impact, friction, clearances, tolerances, alignment, and preloading are likely to all become increasingly important as chain speed increases.

Typical data for one cycle around the loop (seated on load sprocket, exiting load sprocket, in tight chain span, over idler, in tight chain span, entering drive sprocket, seated on drive sprocket, exiting drive sprocket, in loose chain span, entering load sprocket) are shown in Figure 4a and 4b.

There were clear and repeatable spikes at the point where the link leaves the load sprocket and at the point where the link enters the drive sprocket. There were no spikes at either the entry or the exit points on the idler sprocket, indicating that these spikes correspond to transient forces associated with rapid changes in the link tension.

A second and related observation about the data is that the transition from the tight side tension to the loose side tension took place in the space of less than two links at the point of entry onto the drive sprocket. Similarly, the transition from the loose side tension to the tight

side tension took place in less than two links at the point of exit from the load sprocket. These results agree with the experimental observations made by Staments (1951) in his early experiments, and contradict the predictions that would be made by Binder's (1956) analytical model.

IMPACT FORCE

Procedure

The procedure developed to measure the impact force as a roller seats on the sprocket is outlined below.

1. Preload upper chain span. Monitor output from the idler sprocket support load cells.

2. Turn on machine and place resistance across alternator circuit.

3. Configure Bruel & Kjaer 2032 dual channel spectrum analyzer (B&K 2032) to monitor frequency domain response of idler sprocket support load cells.

4. Power the speed photocell. The photocell and the computer controlling the experiment determine the rotational speed of the instrumented sprocket.

5. Warm up test machine for five minutes.

6. A total of 1500 spectra are averaged from both load cells. A spectrum is defined by 2048 points sampled at the Nyquist criterion rate. For this experiment, 4096 points per second were received by the analyzer. While the analyzer is averaging data, the speed photocell is intermittently polled and the rotational speed of the instrumented sprocket is determined.

7. Stop test machine and remove power from the speed photocell. Transfer data from the B&K 2032 to a computer file. Include in the file the time and date of the test, the speed of the instrumented sprocket, and the X,Y pairs (the frequency and the output from the load ring corresponding to this frequency) from the averaged spectra. To complete the next run, these steps are repeated.

The entire test procedure was automated and controlled by an Intel 80286 based personal computer. This facilitated repeatability and consistency. Once an experimental group was completed, the load cells were removed from the test machine, the chain was replaced, the speed was changed, and the calibration was checked. The machine was then reassembled in preparation for the next experimental group.

Impact Data and Discussion

The data collected allow the determination of the impact force spectrum for various chain tensions and instrumented sprocket speeds. The strategy is based on an experimentally determined transfer function approach facilitated by the Bruel & Kjaer 2032 dual channel spectrum analyzer. Typical frequency domain data and results are presented in Figure 5.

To obtain the transfer function, linear behavior was assumed, a known input excitation was applied to the sprocket, and the system response was measured. The transfer function is just the response divided by the input. Following this approach, transfer functions were obtained for both the horizontal and the vertical load cells. In subsequent experiments, the system response was measured, and the input (i.e., the impact force) was determined by dividing the response by the transfer function.

Magnitude of the Impact Force

The impact force data can be presented in a three dimensional plot (see Figure 6) where impact force is shown as a response surface mapped over sprocket speed and chain tension. Raw data are presented in the Appendix.

The impact force ranges from a low value of 6 pounds (800 rpm, 20 pound preload, 57.61 inch pounds of torque transmitted) to a high of 125 pounds (1400 rpm, 70 pound preload, 37.63 inch pounds of torque transmitted). Referring to Figure 6, as the tension in the chain span increases, the impact force also tends to increase. The impact force also tends to increase as the sprocket speed increases. However, neither relationship is monotonic. Data points contrary to these trends are dispersed throughout the space and their location(s) are likely to be related to the specific geometric details of the apparatus (possibly due to linear and/or nonlinear vibration phenomena in the system). This will be the subject of future investigations.

A very steep rise in impact force was observed for increasing sprocket speed in the vicinity of 100 radians/sec and also in the vicinity of 120 radians/sec. We suggest that these data indicate the complexity of the relation between the impact force and the other system variables. Further research into the relation between the impact force and the mode shapes of the chain span, center distances, tension, chain speed, friction, clearances, tolerances, and alignment will be necessary before the impact phenomenon can be fully explained. A detailed analytical study of chain span vibration is presently being conducted by Choi and Johnson at the University of Michigan.

The data can be summarized by an empirical equation obtained by regression analysis, i.e.

$$\text{Impact Force} \approx -.00003\omega^3 T + .012892\omega^2 T - 1.37118\omega T + 47.43351 T + .000746\omega^3 - .25491\omega^2 + 28.02622\omega - 989.466 \qquad (3)$$

where ω is the angular velocity of the sprocket in radians per second and T is the chain tension in pounds. (In these experiments, the instrumented idler sprocket was set in the tight side of the chain span).

The average difference between the impact force as computed by equation (3) and the impact force as measured in the experiment was 1.1068 pounds. Equation (3) is presented graphically in Figure 7.

Angle of Impact

Since the two load cells were mounted on two force members, the angle of the impact force is readily determined. The largest component of impact force was always detected by the vertical load cell. At 800 rpm, the angle of impact was approximately 11° from the vertical. At 1000 rpm, the angle of impact was approximately 13° from the vertical. At 1200 rpm, it was approximately 15.3°. At 1400 rpm, it was approximately 18°. These data indicate that the roller seating process is clearly speed dependent. This might be exploited through the design of special sprocket seat geometries for critical applications. This should be investigated further.

CONCLUSION

The data presented here provide a basis for further investigation in order to develop explicit phenomenological explanations of the behavior of chain drives. The following specific conclusions can be drawn from the data.

- As is typically assumed, under quasi-static conditions, dynamic effects can be

neglected without introducing significant error.

- As chain speed increases, dynamic effects become increasingly important.
- As is the case for belt drives, the average tight side chain tension can be expressed in the classical form of the preload, the driven load, and the load due to centrifugal force with only modest error over a wide range of linear chain speeds.
- The tension in a chain link increases very rapidly as the link exits the driven sprocket. The increase from loose side to tight side average tension occurs over less than two sprocket teeth.
- The tension in a chain link decreases very rapidly as the link enters the drive sprocket. The decrease from tight side to average loose side tension occurs over less than two sprocket teeth.
- Transient spikes are present in the tension data at the point where the link exits the driven sprocket and at the point where the link enters the driven sprocket.
- Impact force tends to increase as chain tension increases, however the relationship is not monotonic.
- Impact force tends to increase as chain speed increases, however the relationship is not monotonic.
- For a chain traveling in the horizontal direction, the vertical component of the impact force is much larger than the horizontal component.
- The magnitude of the horizontal component of the impact force increases more rapidly than the magnitude of the vertical component as the chain speed increases, indicating that the angle of impact (as measured from a vertical line) increases as chain speed increases.

ACKNOWLEDGMENTS

The authors gratefully acknowledge the support of the National Science Foundation through grants no. MSM-88-12957 and MSS-89-06293. We also wish to acknowledge the value of discussions with Messrs. S. Peterson, R. McReynolds, and G. Walker of Vanderbilt University, Messrs. N. Miller and F. Rasmussen of Bruel and Kjaer Instruments, Mr. R. Carroll of Sign Management Consultants, and Mr. K. Goodwin of Sverdrop Technologies.

REFERENCES

Beikmann, R. S., Perkins, N. C., and Ulsoy, A. G., 1992, "Free Vibration Analysis of Automotive Serpentine Belt Accessory Drive Systems," Proceedings of the 1992 CSME Mechanical Engineering Forum, Montreal, Canada, June, 1992, pp. 118-123.

Binder, R. C., 1956, Mechanics of the Roller Chain Drive, Prentice-Hall, Englewood Cliffs, NJ.

Chen, C-K, and Freudenstein, F., 1988, "Toward a More Exact Kinematics of Roller Chain Drives," Trans. ASME J. Mechanisms, Transmissions and Automation in Design, Volume 110, No. 3, pp. 269-275.

Choi, W. and Johnson, G. E., 1992a, Vibration of Roller Chain Drives at Low, Medium and High Operating Speeds, MEAM Technical Report Number 92-08, University of Michigan, Ann Arbor, Michigan.

Choi, W. and Johnson, G. E., 1992b, Transverse Vibrations of a Roller Chain Drive with Tensioner, MEAM Technical Report Number 92-09, University of Michigan, Ann Arbor, Michigan.

Conwell, J. C., 1989, An Examination of Transient Forces in Roller Chain Drives, Ph.D. Dissertation, Vanderbilt University, December 1989.

Eldiwany, B. H. and Marshek, K. M., 1984, "Experimental Load Distributions for Double Pitch Steel Roller Chains on Steel Sprockets," Mechanism and Machine Theory, Volume 19, Number 6, pp. 449-457.

Gerbert, G., et al, 1978, "Load Distribution in Timing Belts," Trans. ASME J. Mechanical Design, V. 100, pp. 208-215.

Gerbert, G., 1989, "Tooth Action in Chain and Timing Belt Drives," Proceedings of the International Power Transmission and Gearing Conference, Volume 1, ASME, Book 10288A - 1989, pp 81

Kim, M. S., 1990, Dynamic Behavior of Roller Chain Drives at Moderate and High Speeds, Ph.D. dissertation, The University of Michigan, 1990, 122 pp

Kim, M. S., and Johnson,G. E., 1992a, Mechanics of Roller Chain-Sprocket Contact, MEAM Technical Report Number 92-06, University of Michigan, Ann Arbor, Michigan.

Kim, M. S., and Johnson, G. E., 1992b, A General Multi-Body Dynamic Model to Predict the Behavior of Roller Chain Drives at Moderate and High Speeds, MEAM Technical Report Number 92-07, University of Michigan, Ann Arbor, Michigan.

Marshek, K. M., 1978, "On the Analyses of Sprocket Load Distribution," Mechanism and

Machine Theory, Volume 14, pp. 135-139.

Mote, C. D. , Jr., 1965, "A Study of Band Saw Vibrations," Journal of the Franklin Institute, Vol. 279, no. 6, pp. 430-444.

Naji, M. and Marshek, K. M., 1983a, "Analysis of Sprocket Load Distribution," Mechanism and Machine Theory, Volume 18, Number 5, pp. 349-356.

Naji, M. and Marshek, K. M., 1983b, "Experimental Determination of the Roller Chain Load Distribution," Trans. ASME J. Mechanisms, Transmissions and Automation in Design, Volume 105, pp. 331-338.

Radzimovsky, E. I., 1955, "Eliminating Pulsations in Chain Drives," Product Engineering, Volume 26, pp. 153-157.

Staments, W. K., 1951, "Dynamic Loading of Chain Drives," Trans. ASME, July 1951, pp. 655-665.

Turnbull, S. R., and Fawcett, J. N., "An Approximate Kinematic Analysis of the Roller Chain Drive," Proceedings of the Fourth World Congress on Theory of Machines and Mechanisms, pp. 907-911.

Veikos, N. C. and Freudenstein, F. 1992a, "On the Dynamic Analysis of Roller Chain Drives : Part 1- Theory", Mechanism Design and Synthesis, DE-vol. 46, edited by Kinzel et al, ASME, NY, 1992, pp.431-438.

Veikos, N. C. and Freudenstein, F., 1992b, "On the Dynamic Analysis of Roller Chain Drives: Part 2,", Mechanism Design and Synthesis, DE-vol. 46, edited by Kinzel et al, ASME, NY, 1992, pp.439-450.

Wang, K. W., 1992, "On the Stability of Chain Drive Systems Under Periodic Sprocket Oscillations," Trans. ASME J. Vibration and Acoustics, Vol. 114, pp 119 - 126.

Wang, K. W., et al, 1992, "On the Impact Intensity of Vibrating Axially Moving Roller Chains," Trans. ASME J. Vibration and Acoustics, Vol. 114, pp 397 - 403.

APPENDIX

This appendix lists the data collected during the experiments described in this paper. The data are grouped according to the rotational speeds of the instrumented sprocket (800, 1000, 1200 and 1400 RPM).

The following terms are used throughout this appendix:

Sprocket Speed - The rotational speed of the instrumented sprocket.

Preload - The amount of preload, in pounds, placed in the upper chain span prior to each test.

Torque - The amount of torque, in inch-pounds, transmitted by the chain drive during an experimental run.

Chain Force - The average chain force, in pounds, determined from the data collected during the experiment.

Impact Force - The impact force, in pounds, measured during the experiment.

800 RPM Data

Sprocket Speed (RPM)	Preload (lbs)	Torque (in-lbs)	Chain Force (lbs)	Impact Force (lbs)
798.112	20	27.61	36.9733	15.397
796.937	20	32.19	38.9635	15.06
795.367	20	37.63	41.912	13.556
793.593	20	41.77	44.091	11.564
791.323	20	45.99	46.824	10.815
788.630	20	57.61	51.927	6.82
798.277	30	27.61	47.1751	12.222
797.272	30	32.19	48.732	13.129
795.785	30	37.63	50.941	12.493
793.988	30	41.77	53.912	11.163
792.071	30	45.99	56.811	13.409
789.776	30	57.61	62.127	13.11
798.234	40	27.61	57.223	16.714
796.941	40	32.19	58.744	17.897
795.364	40	37.63	60.983	17.29
793.661	40	41.77	64.012	16.18
791.477	40	45.99	66.932	19.23
789.110	40	57.61	72.141	18.23
797.871	50	27.61	67.119	21.45
796.499	50	32.19	68.814	22.02
794.893	50	37.63	70.721	18.64
793.151	50	41.77	74.132	17.311
790.735	50	45.99	76.855	9.02
788.250	50	57.61	83.512	8.31
797.742	60	27.61	77.252	21.443
796.204	60	32.19	79.242	21.737
794.828	60	37.63	80.933	19.001
792.944	60	41.77	85.311	19.325
790.366	60	45.99	87.144	19.413
787.771	60	57.61	94.030	13.904
797.185	70	27.61	87.523	25.02
795.900	70	32.19	89.621	24.504
794.231	70	37.63	91.521	20.951
792.831	70	41.77	95.442	23.522
790.549	70	45.99	95.427	23.746
787.889	70	57.61	105.02	15.65

1000 RPM Data

Sprocket Speed (RPM)	Preload (lbs)	Torque (in-lbs)	Chain Force (lbs)	Impact Force (lbs)
787.151	20	27.61	38.2463	27.74
984.975	20	32.19	40.1735	28.708
981.945	20	37.63	43.158	29.686
979.170	20	41.77	45.731	28.336
975.620	20	45.99	48.321	25.277
971.343	20	57.61	53.6181	21.924
985.105	30	27.61	48.6321	26.186
983.685	30	32.19	50.921	21.294
981.523	30	37.63	53.421	34.462
978.097	30	41.77	54.921	35.249
974.667	30	45.99	57.921	32.911
971.535	30	57.61	65.001	31.308
985.431	40	27.61	58.451	29.664
982.476	40	32.19	61.031	22.244
980.697	40	37.63	63.151	29.984
978.569	40	41.77	65.314	12.523
975.080	40	45.99	68.314	15.416
972.658	40	57.61	74.511	13.352
984.554	50	27.61	68.215	14.562
982.440	50	32.19	70.421	36.023
980.160	50	37.63	73.851	46.409
977.137	50	41.77	74.801	25.838
973.362	50	45.99	78.711	19.226
970.344	50	57.61	83.923	27.961
984.290	60	27.61	78.316	34.432
982.329	60	32.19	80.164	28.004
979.795	60	37.63	84.631	36.06
977.543	60	41.77	85.117	31.795
972.709	60	45.99	87.932	40.827
969.911	60	57.61	94.520	43.731
983.877	70	27.61	88.724	55.837
981.877	70	32.19	90.051	54.575
979.417	70	37.63	94.211	48.641
976.445	70	41.77	94.991	46.477
972.867	70	45.99	96.541	35.946
969.584	70	57.61	106.301	37.212

1200 RPM Data

Sprocket Speed (RPM)	Preload (lbs)	Torque (in-lbs)	Chain Force (lbs)	Impact Force (lbs)
1147.518	20	27.61	39.8823	35.561
1145.014	20	32.19	41.8515	39.655
1142.779	20	37.63	44.745	30.544
1139.911	20	41.77	47.728	27.713
1137.196	20	45.99	49.868	15.145
1133.737	20	57.61	55.7145	6.635
1145.543	30	27.61	49.5311	64.174
1142.647	30	32.19	52.248	61.139
1140.379	30	37.63	53.921	58.285
1138.062	30	41.77	57.311	53.073
1135.036	30	45.99	59.767	49.410
1131.848	30	57.61	65.237	43.227
1145.008	40	27.61	60.354	79.911
1142.245	40	32.19	61.531	76.659
1140.062	40	37.63	64.318	72.985
1136.959	40	41.77	68.012	65.949
1134.015	40	45.99	70.317	64.937
1130.475	40	57.61	74.921	43.651
1144.116	50	27.61	70.121	127.842
1141.733	50	32.19	70.991	103.44
1138.906	50	37.63	74.815	100.207
1136.108	50	41.77	77.814	82.131
1133.149	50	45.99	80.824	70.401
1129.767	50	57.61	85.012	84.842
1143.221	60	27.61	80.041	120.5855
1140.979	60	32.19	80.513	93.685
1138.296	60	37.63	85.210	90.379
1135.234	60	41.77	86.999	89.565
1132.116	60	45.99	89.931	76.734
1129.331	60	57.61	96.130	74.310
1142.706	70	27.61	91.423	116.375
1139.363	70	32.19	92.131	105.120
1136.047	70	37.63	94.721	91.729
1132.624	70	41.77	97.241	93.129
1129.869	70	45.99	101.421	83.282
1126.615	70	57.61	106.017	78.072

1400 RPM Data

Sprocket Speed (RPM)	Preload (lbs)	Torque (in-lbs)	Chain Force (lbs)	Impact Force (lbs)
1335.587	20	27.61	41.7975	39.557
1332.206	20	32.19	43.5675	43.21
1331.098	20	37.63	46.5605	39.585
1328.077	20	41.77	49.644	43.242
1324.237	20	45.99	51.578	49.887
1320.399	20	57.61	57.603	39.649
1333.468	30	27.61	52.3011	51.835
1331.762	30	32.19	54.176	51.984
1328.783	30	37.63	56.213	57.701
1326.847	30	41.77	58.920	52.481
1323.883	30	45.99	61.375	66.826
1319.846	30	57.61	67.922	58.616
1333.504	40	27.61	61.542	55.465
1331.941	40	32.19	63.211	54.755
1328.783	40	37.63	65.911	60.221
1326.622	40	41.77	69.311	56.55
1322.981	40	45.99	71.042	63.79
1318.839	40	57.61	76.711	61.296
1332.007	50	27.61	72.850	59.075
1330.167	50	32.19	73.644	61.659
1326.411	50	37.63	76.429	56.310
1323.742	50	41.77	79.714	64.661
1320.642	50	45.99	82.013	52.481
1317.268	50	57.61	87.940	54.365
1330.213	60	27.61	81.623	74.07
1327.251	60	32.19	84.515	77.231
1325.282	60	37.63	87.361	89.610
1322.683	60	41.77	88.930	103.816
1320.295	60	45.99	92.341	91.705
1315.979	60	57.61	97.581	95.555
1330.152	70	27.61	91.854	96.82
1328.026	70	32.19	94.131	107.392
1323.791	70	37.63	96.250	125.557
1322.522	70	41.77	99.112	123.489
1318.082	70	45.99	101.832	106.812
1314.898	70	57.61	106.821	100.832

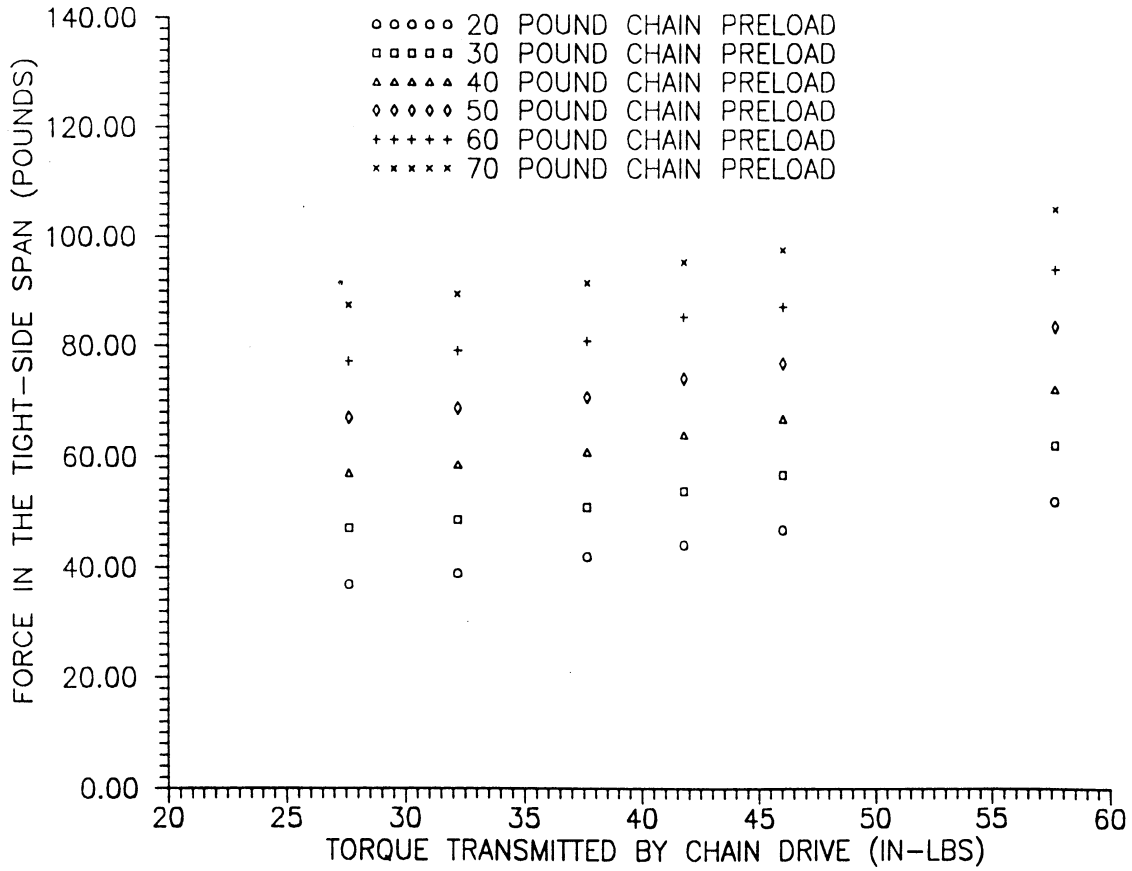

Figure 1a. Time averaged force in the tight side of the chain as a function of transmitted torque and chain preload for a nominal instrumented sprocket speed of 800 rpm

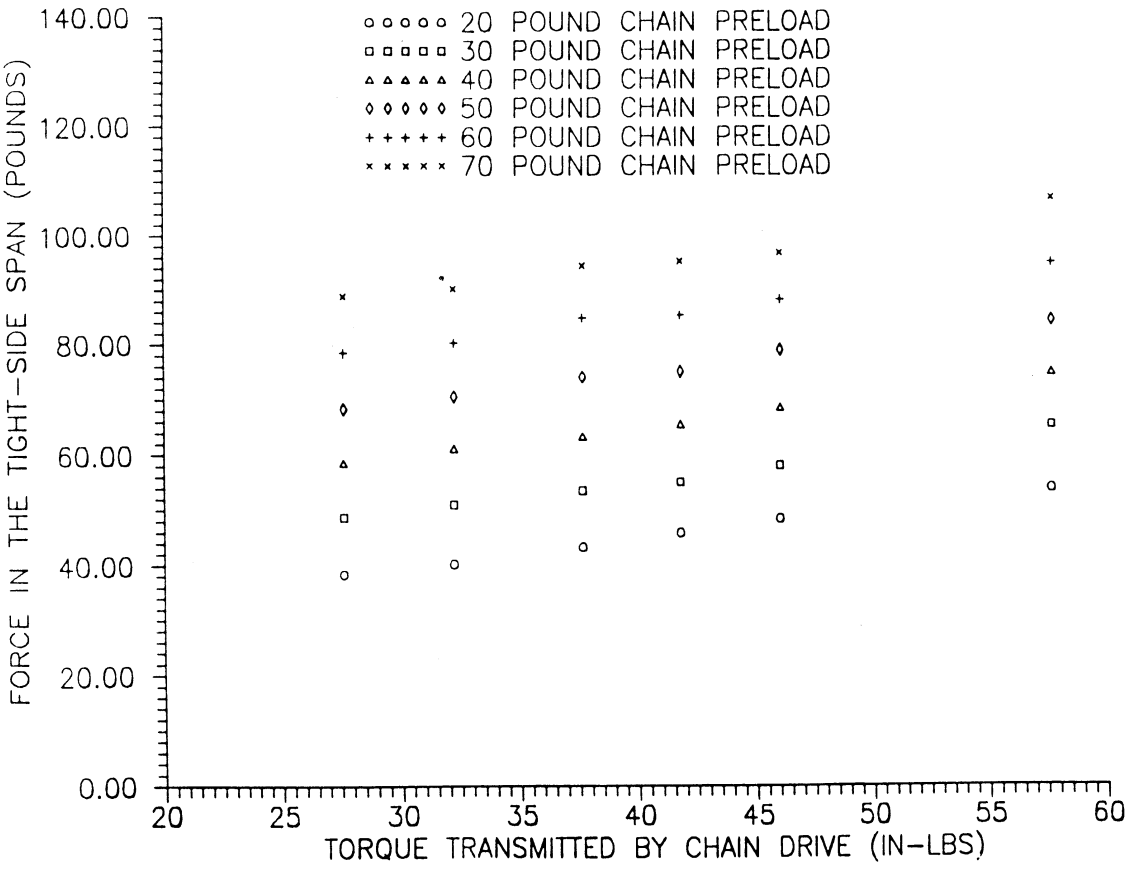

Figure 1b. Time averaged force in the tight side of the chain as a function of transmitted torque and chain preload for a nominal instrumented sprocket speed of 1000 rpm

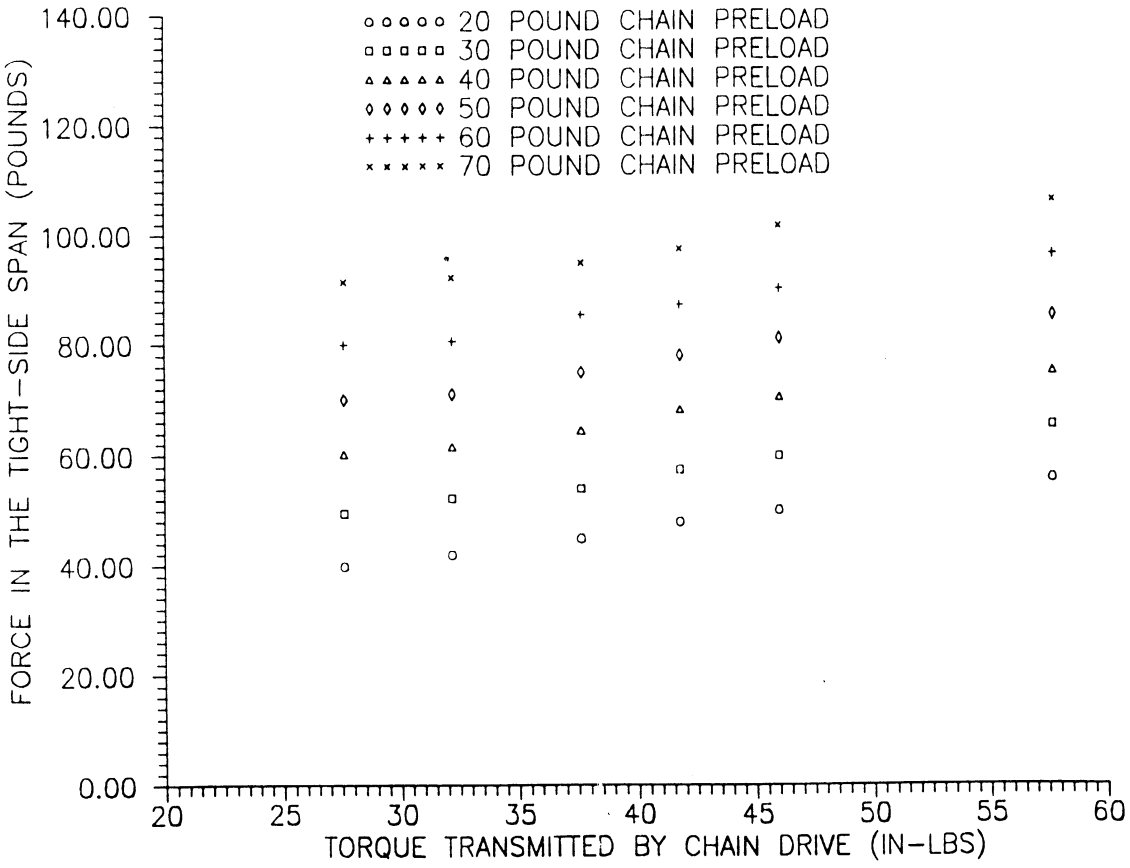

Figure 1c. Time averaged force in the tight side of the chain as a function of transmitted torque and chain preload for a nominal instrumented sprocket speed of 1200 rpm

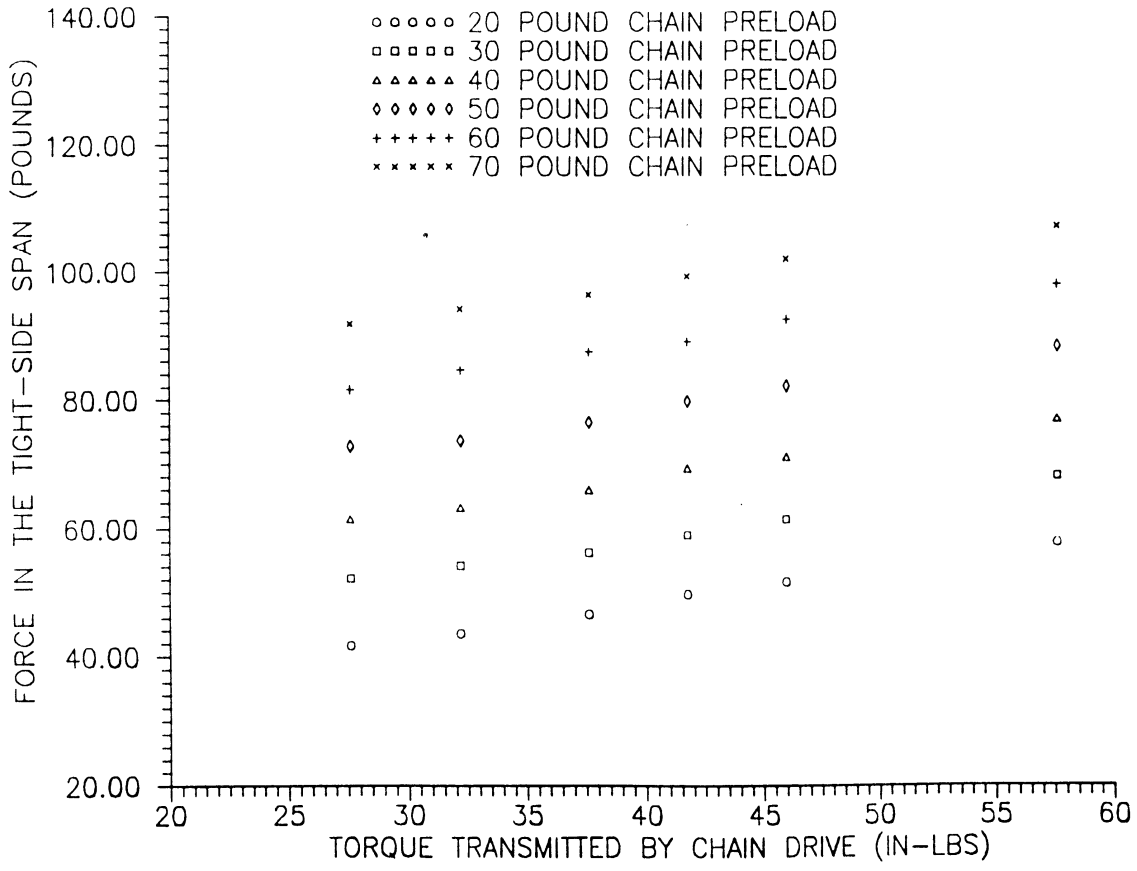

Figure 1d. Time averaged force in the tight side of the chain as a function of transmitted torque and chain preload for a nominal instrumented sprocket speed of 1400 rpm

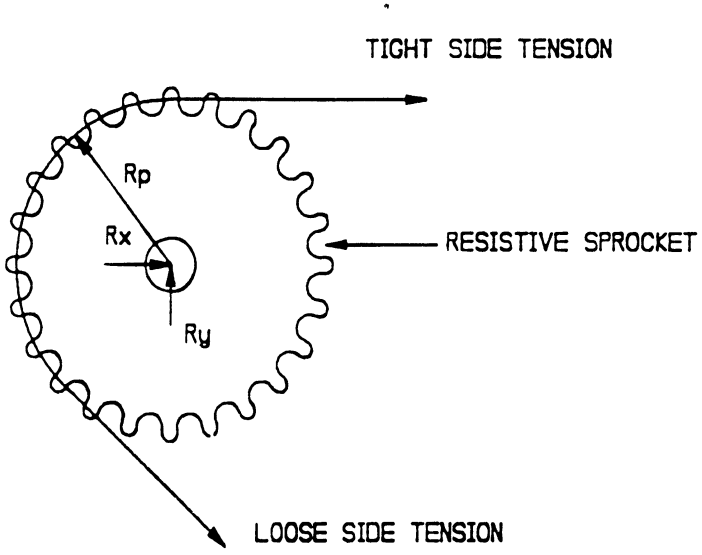

Figure 2. Free body diagram of driven sprocket.

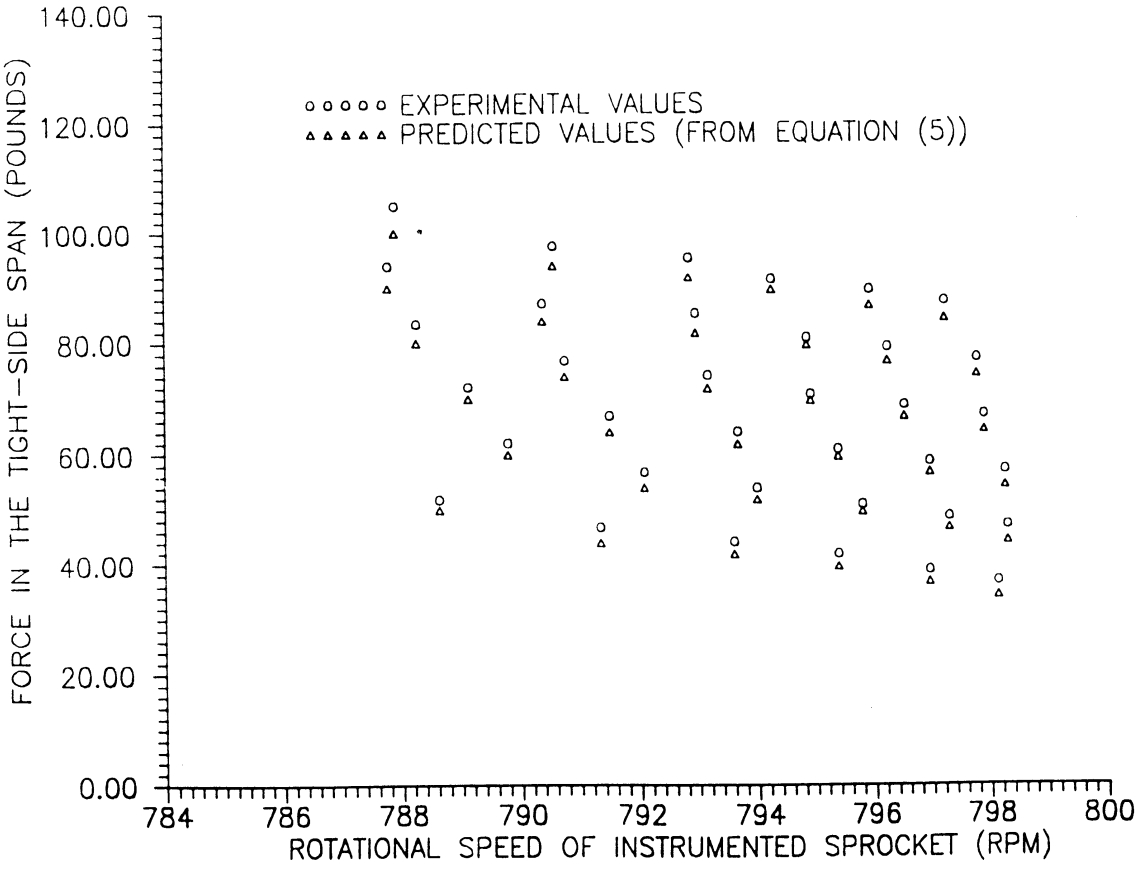

Figure 3a. Experimentally determined tight side chain tension compared to tight side chain tension calculated by Equation (1) for a nominal instrumented sprocket speed of 800 rpm.

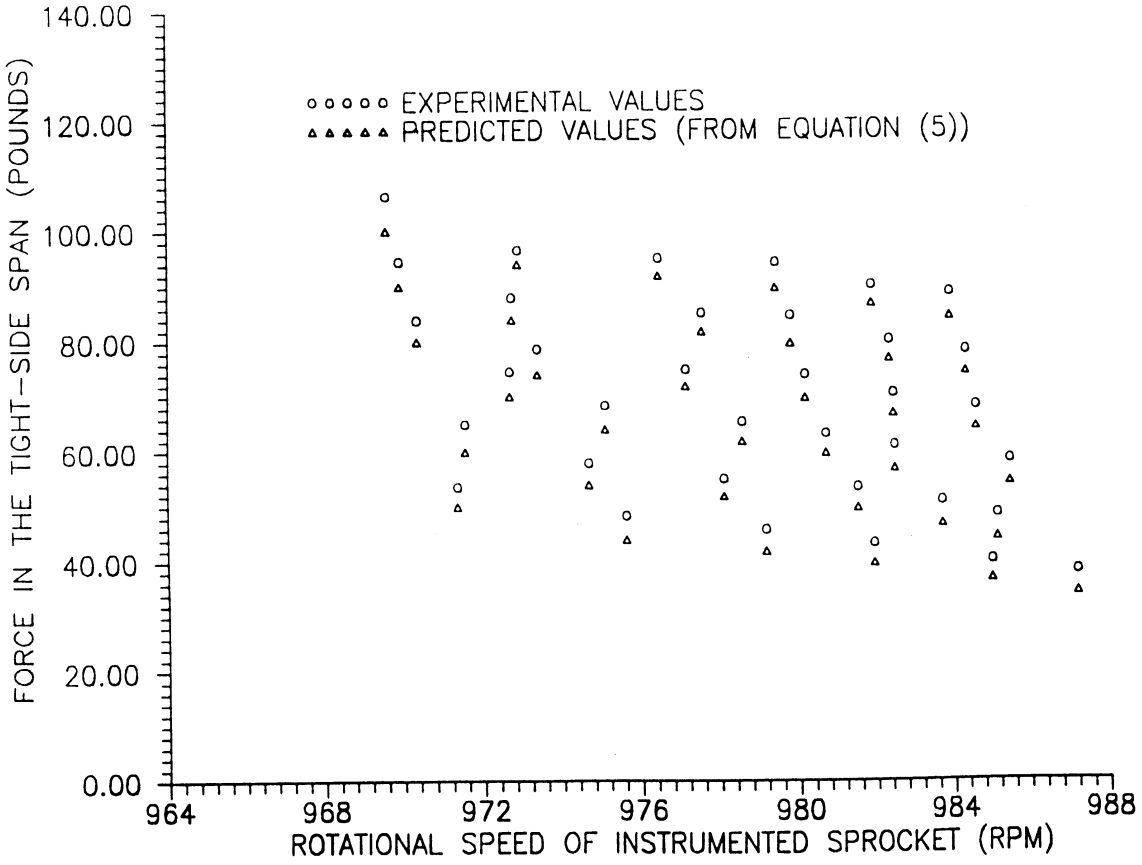

Figure 3b. Experimentally determined tight side chain tension compared to tight side chain tension calculated by Equation (1) for a nominal instrumented sprocket speed of 1000 rpm.

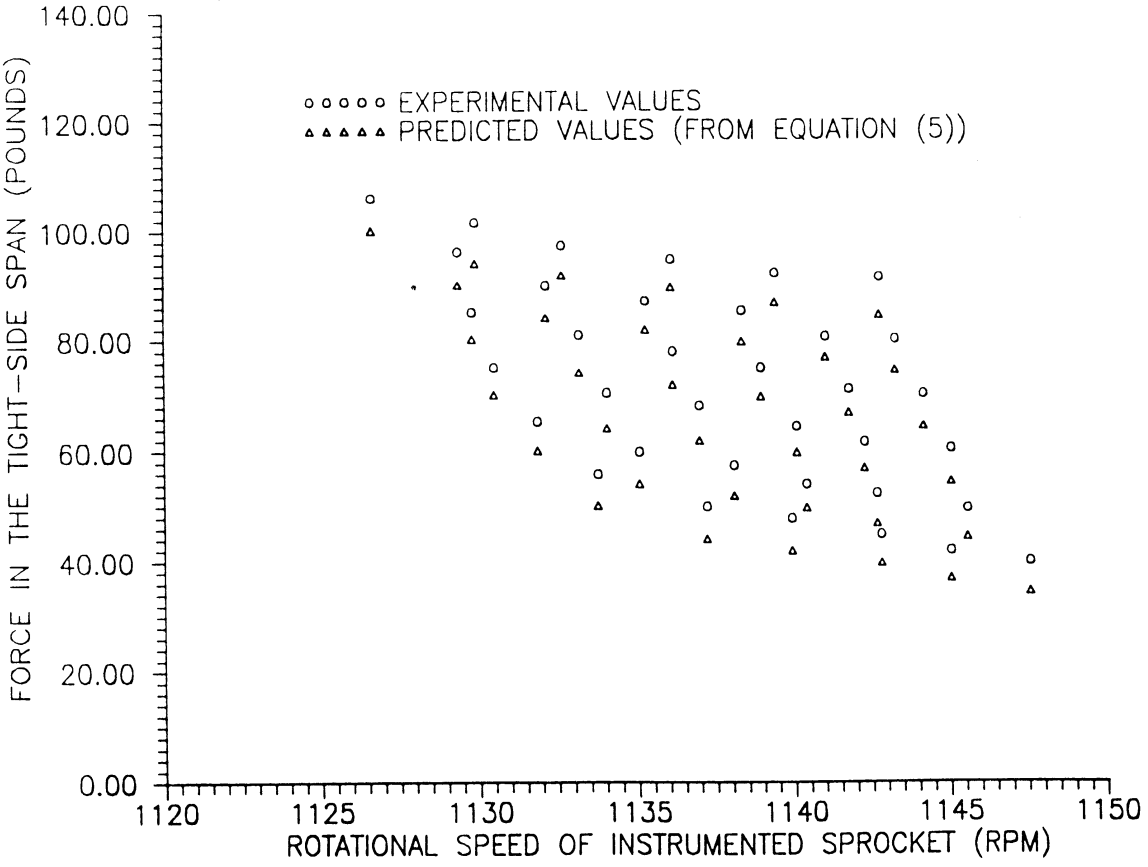

Figure 3c. Experimentally determined tight side chain tension compared to tight side chain tension calculated by Equation (1) for a nominal instrumented sprocket speed of 1200 rpm.

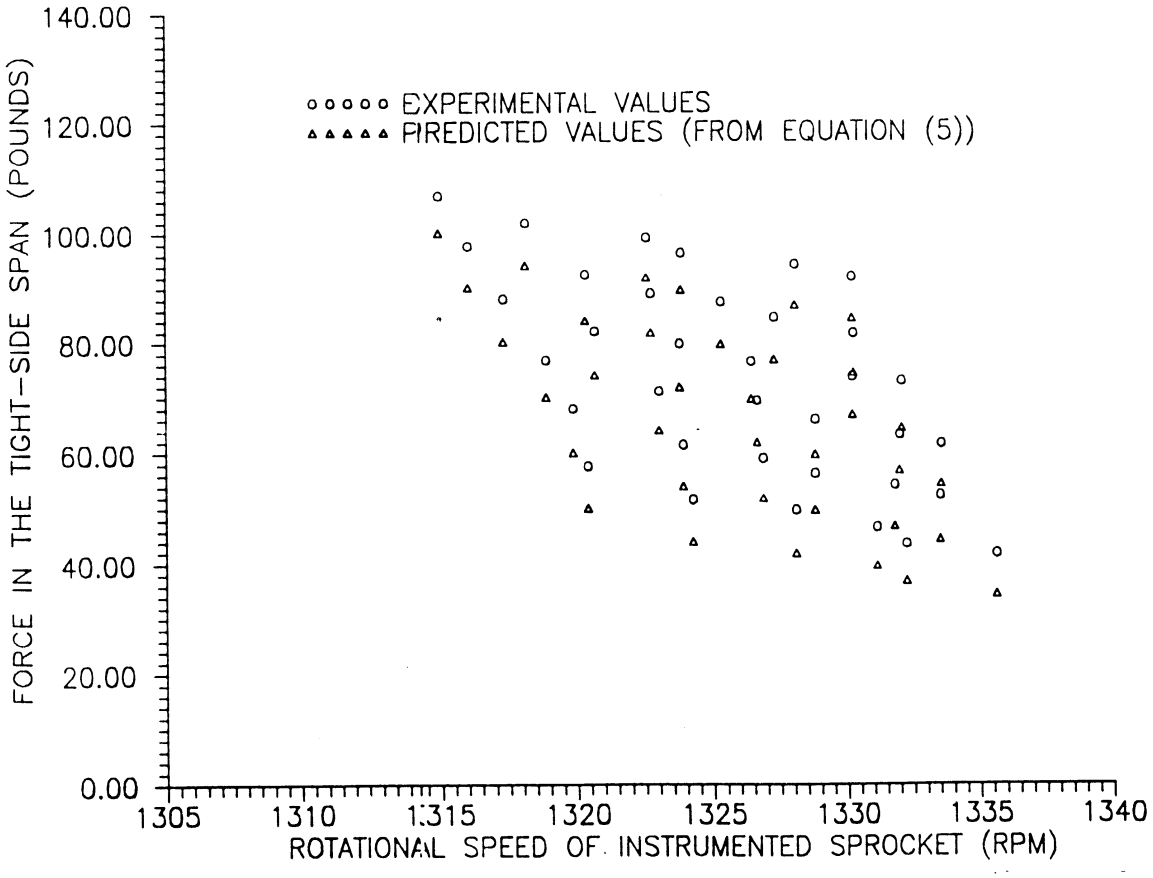

Figure 3d. Experimentally determined tight side chain tension compared to tight side chain tension calculated by Equation (1) for a nominal instrumented sprocket speed of 1400 rpm.

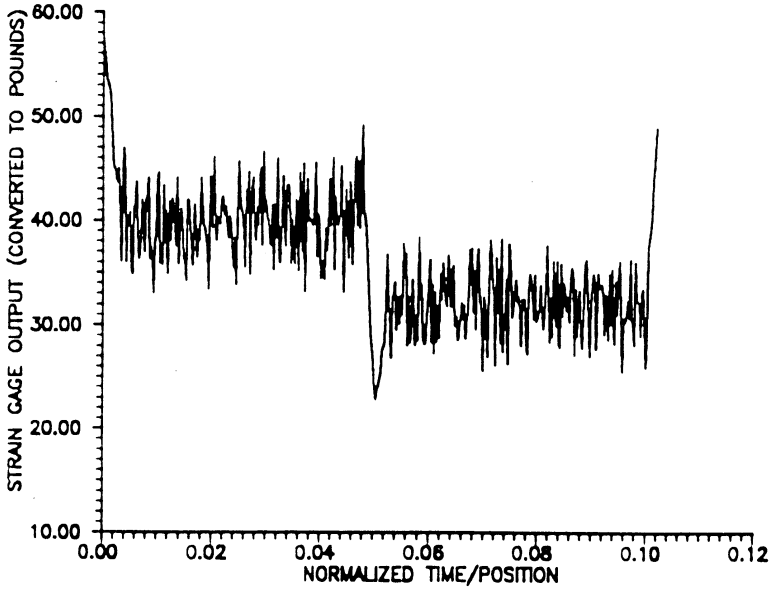

Figure 4a. Typical output from strain gage mounted on link side plate over one complete cycle around the loop.

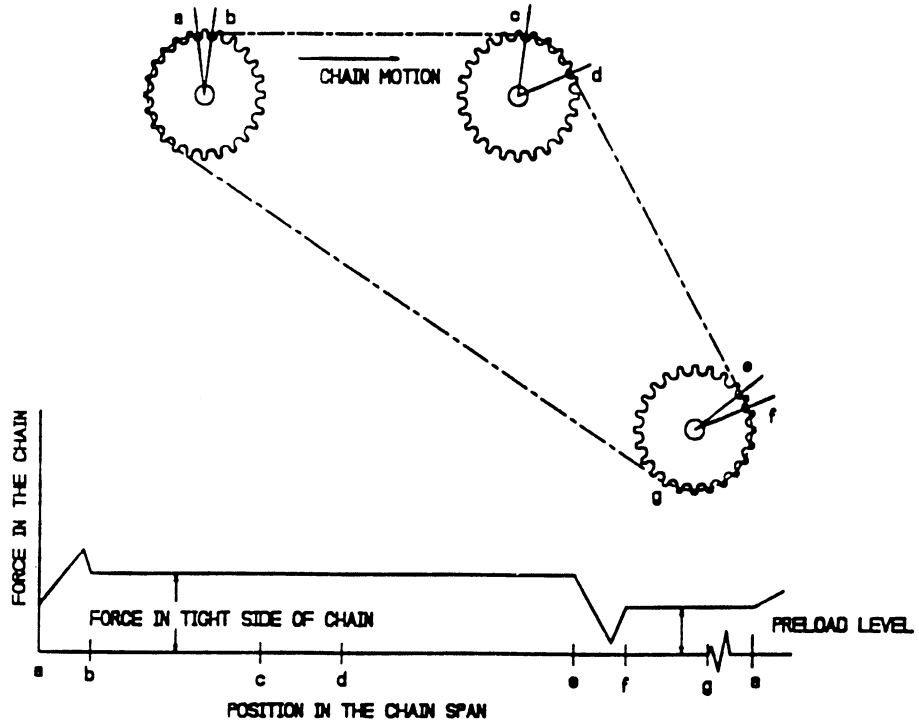

Figure 4b. Typical time averaged chain force as a function of position in the chain span.

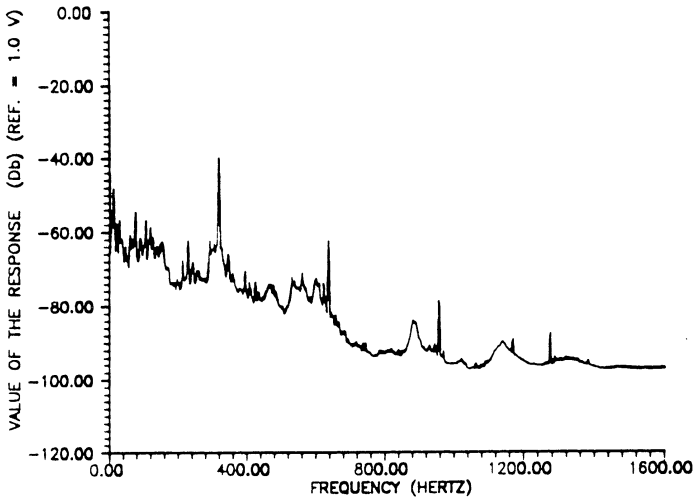

Figure 5a. Typical experimentally measured output spectrum from vertical load cell.

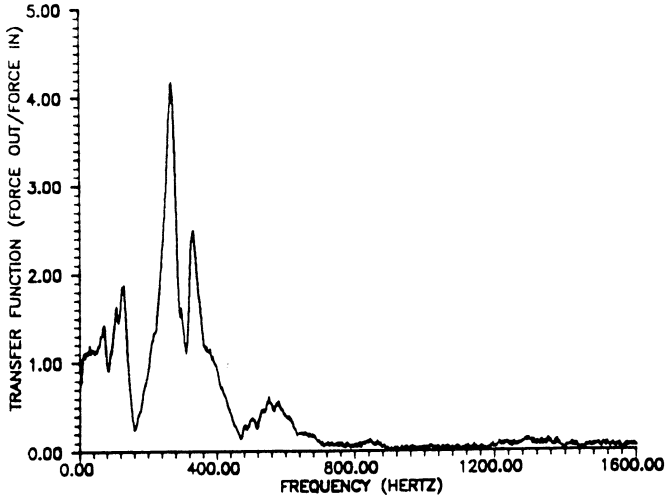

Figure 5b. Vertical load cell transfer function.

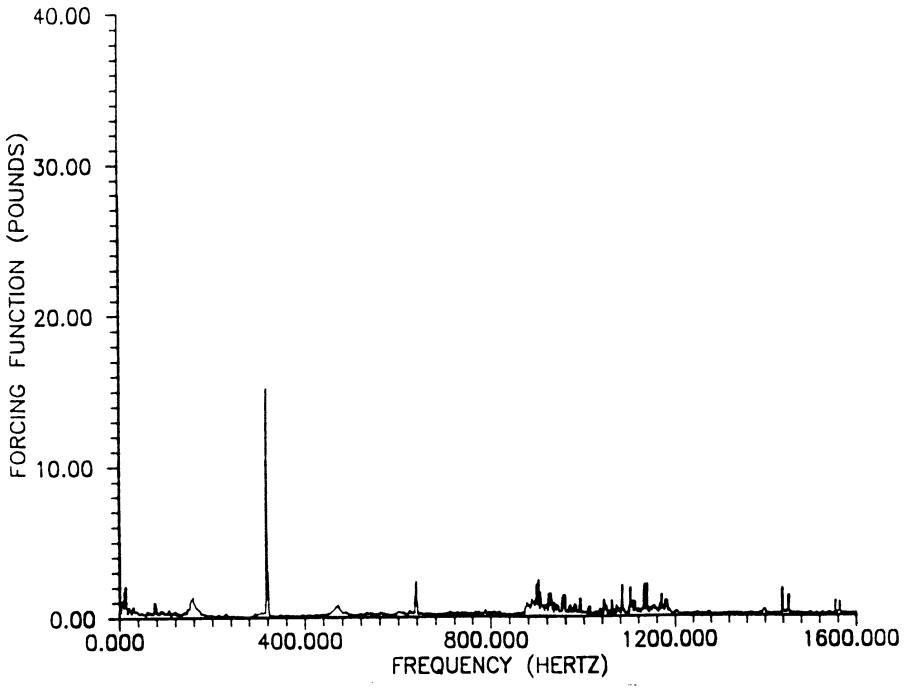

Figure 5c. Typical spectrum of the force applied to the sprocket by the rollers.

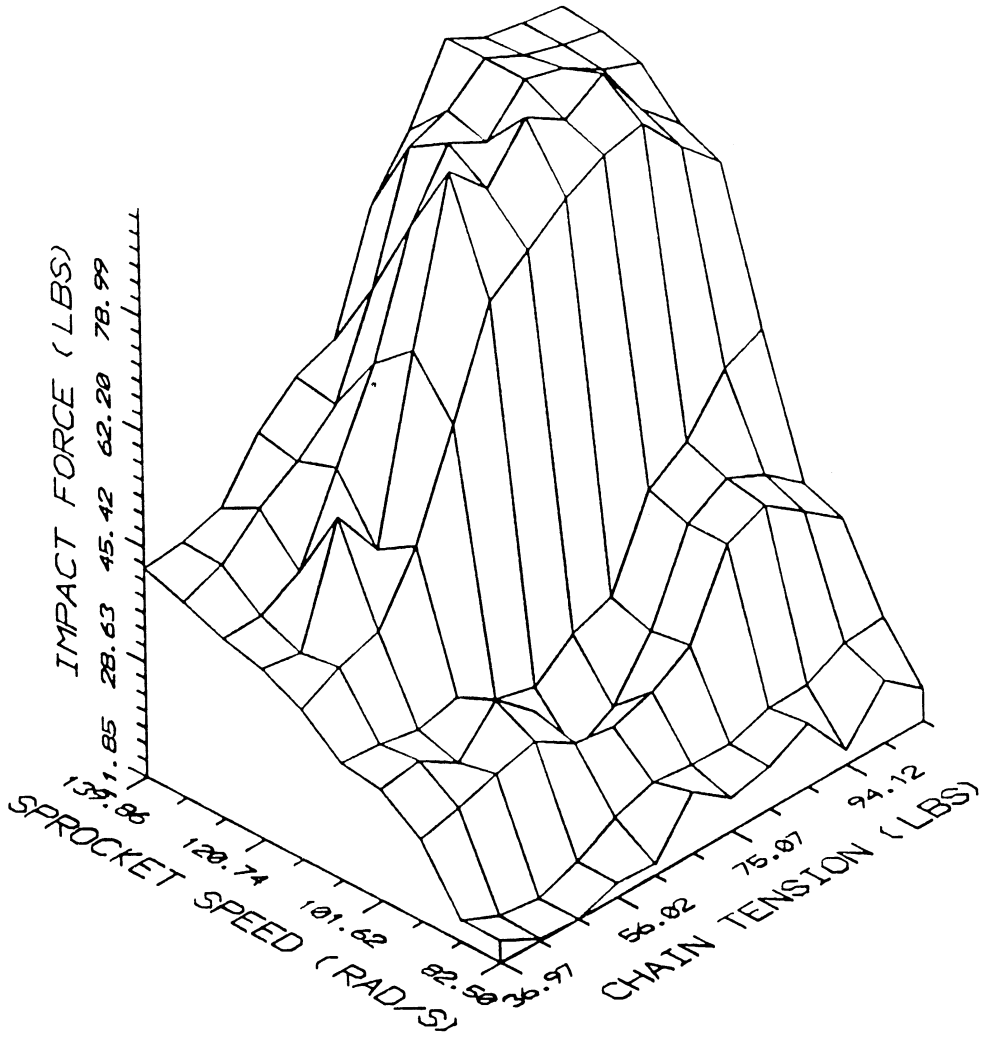

Figure 6. Experimentally measured impact force as a function of sprocket speed and chain tension.

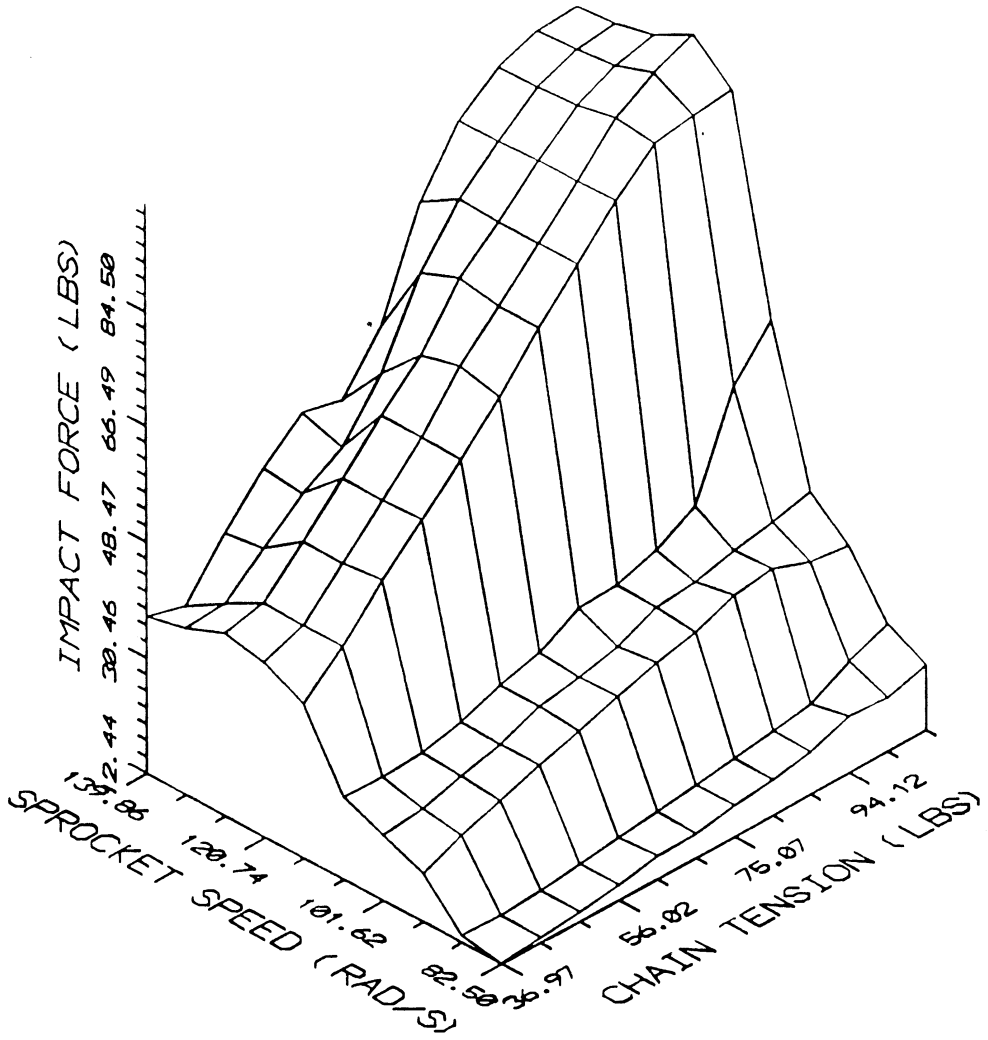

Figure 7. Impact force as a function of sprocket speed and chain tension as predicted by Equation (3).

THE UNIVERSITY OF MICHIGAN

DATE DUE

10-3 13:55